



# Journal of Applied and Computational Mechanics



Research Paper

## Shear-flexure Interaction Frame Model on Kerr-type Foundation for Analysis of Non-ductile RC Members on Foundation

Suchart Limkatanyu<sup>1</sup>, Worathep Sae-Long<sup>2</sup>, Nattapong Damrongwiriyanupap<sup>3</sup>, Thanongsak Imjai<sup>4</sup>,  
Preeda Chaimahawan<sup>5</sup>, Piti Sukontasukkul<sup>6</sup>

<sup>1</sup> Department of Civil and Environmental Engineering, Prince of Songkla University, Songkhla, 90112, Thailand, Email: suchart.l@psu.ac.th

<sup>2</sup> Civil Engineering Program, School of Engineering, University of Phayao, Phayao, 56000, Thailand, Email: worathep.sa@up.ac.th

<sup>3</sup> Civil Engineering Program, School of Engineering, University of Phayao, Phayao, 56000, Thailand, Email: nattapong.da@up.ac.th

<sup>4</sup> School of Engineering and Technology, Walailak University, Nakhorn Si Thammarat, 80160, Thailand, Email: thanongsak.im@wu.ac.th

<sup>5</sup> Civil Engineering Program, School of Engineering, University of Phayao, Phayao, 56000, Thailand, Email: preeda.ch@up.ac.th

<sup>6</sup> Construction and Building Materials Research Center, Department of Civil Engineering, King Mongkut's University of Technology North Bangkok, Bangkok, 10800, Thailand, Email: piti.s@eng.kmutnb.ac.th

Received January 03 2022; Revised February 24 2022; Accepted for publication February 28 2022.

Corresponding author: W. Sae-Long (worathep.sa@up.ac.th)

© 2022 Published by Shahid Chamran University of Ahvaz

**Abstract.** In the present day, non-ductile reinforced concrete (RC) members have still appeared in certain parts of the existing old buildings and bridges. These structures always exhibit shear failure when they have been subjected to seismic loading, resulting in a complicated problem for studying or simulating the behaviors of these structures. The soil-structure interaction is a part of these problems that are of interest and motivated in the current study. Therefore, this paper proposes a novel frame model on the Kerr-type foundation with the inclusion of the shear-flexure interaction for the analysis of the non-ductile RC members resting on the foundation. The proposed model is derived from the displacement-based formulation together with the Timoshenko beam theory. The effects of shear-flexure interaction are taken into account in the proposed model through the shear constitutive law. Finally, two numerical simulations are used to assess the capability, accuracy, and efficiency of the proposed model to characterize non-ductile RC members resting on the foundation. Furthermore, these simulations demonstrate the impact of the shear-flexure interaction on the responses of non-ductile RC members on the foundation.

**Keywords:** Non-ductile RC member, Shear model, Kerr-type foundation, Virtual displacement principle, Finite element.

### 1. Introduction

Soil-structure interactions have been an interesting topic in the engineering fields, which have an impact on both the economy and the safety of the structures and foundations, especially in construction projects. Furthermore, this topic has resulted in several engineering applications in the modern era, such as highway pavement [1-2], underground tunnels [3-4], railway tracks [5-6], pipelines [7], and micro/nanotechnology [8-10], among others. To deeply understand the static and dynamic behaviors of these interaction problems, reliable models are desired to represent the sophisticated characteristics of the interaction between the structures and foundations. As a result, several researchers aim to develop and propose numerical structural models on the foundation that are verified by experiments and simulations [11-18]. Among these models, they can be grouped into two major approaches, namely, (a) the continuous medium model [18-20] and (b) the discrete subgrade spring model [21-23]. For the first approach, the continuous medium model [18-20] can represent the comprehensive responses that vary within the structural system on the foundation. However, this model approach is not very popular due to the intricate boundary problems involved in obtaining the solutions [24]. This leads to several problems and troublesomeness in engineering practice. To overcome the limitations of the continuous model, the subgrade model [21-23] is an alternative approach to represent the interaction between the foundation and structures. This model approach strikes a balance between discretization and accuracy and is appropriate for large-scale systems, resulting in a popular approach for applying to soil-structure interaction problems [25-30]. Therefore, this study employs the concept of the discrete subgrade model to develop the frame model on the foundation model for the analysis of the structural members resting on the foundation.

Among the subgrade foundation models, the Winkler foundation model [31] is the fundamental foundation model, which represents the sophisticated characteristics of soil/foundation with 1-D independent springs attached along with the structural members. Based on this foundation model, the foundation springs are addressed with only one subgrade modulus. As a result, this foundation model is defined as a "one-parameter" foundation model. The Winkler foundation's fundamental assumption is



that each foundation spring model is independent and non-interactive with itself. Based on this hypothesis, there are discontinuous responses obtained from this model approach as widely found in the literature [25-30]. To overcome these drawbacks of the Winkler foundation model, a series of two-parameter foundation models [32-35] and three-parameter foundation models [36-37] is proposed. As its name implies, the conceptual coupling among the Winkler springs is considered and accounted for in these foundation models based on the different mediums as represented by the additional parameters. The Kerr-type foundation [37] is one of the three-parameter foundation models [36-37], which stems from the Winkler foundation [31] and Pasternak foundation [33]. The foundation medium is simulated with two Winkler spring layers attached to the incompressible shear layer. This foundation model is of interest for modeling the sophisticated characteristics of the foundation-structure interaction since it can reliably capture the degree of foundation-surface continuity inside and outside the load regions of the structure-foundation systems [38]. As a result, the Kerr-type foundation has been employed in solving soil-structure interaction problems in the past two decades [38-43]. For example, Cai et al. [39] studied the free vibration behaviors of the cylindrical panel system on the foundation based on the notion of the Kerr-type foundation. Avramidis and Morfidis [40] proposed parametric studies of the beam on the elastic foundation with an infinite or finite length based on the Kerr-type foundation model compared to the Winkler foundation and two-parameter foundation. Limkatanyu et al. [38] presented the exact element stiffness matrix of the Euler-Bernoulli beam on the Kerr-type foundation for the static investigation of the responses of the beam problems resting on the foundation. Zhang et al. [41] employed the Kerr-type foundation to investigate the buckling characteristics of a beam bonded to an elastic foundation. Wang et al. [42] used the idea of the Euler-Bernoulli beam on the Kerr-type foundation to study the settlement of low reinforced embankments on a soft foundation. Jena et al. [43] studied the free vibration of a functionally graded (FG) porous beam embedded in the Kerr foundation based on the shifted Chebyshev polynomial-based Rayleigh-Ritz method and Navier's technique. All the mentioned studies [38-43] have well demonstrated the ability to represent the soil-structure interaction of the Kerr-type model. Therefore, this work aims to develop the frame-foundation model based on the concept of the Kerr-type foundation.

Regarding the non-ductile reinforced concrete (RC) members, these structures have been found in the old existing buildings and bridges designed and constructed before the enforcement of the modern seismic design codes (before the 1980s). These members (with small span-to-depth ratios) always fail in non-ductile failures (brittle failures), i.e., shear failures and/or flexure-shear failures, due to the insufficient details of the transverse reinforcement. As a result, the influence of shear also plays an important role in the control of failure among these members [44-48]. In terms of the engineering design for the RC structures, these non-ductile failures should be avoided [49]. However, it is well known that the mechanism related to the shear effect is highly complicated [44-51]. Thus, several strategies [52-53] to account for the shear behavior within the structural models have been developed and proposed, as excellently reported by Ceresa et al. [54]. For example, the Modified Compression Field Theory (MCFT) of Vecchio and Collins [52] is a technique that can capture the in-plane shear and axial stresses by considering the equilibrium, compatibility, and material constitutive relations and then expressing them through the average stresses and average strains at the fiber-section level. The truss analogy [53] is the method that considers the shear behavior equivalent to the truss model. The shear responses of this approach can be obtained from the strut-and-tie model, etc.

In addition to the influence of shear, several studies and experiments [44, 45, 55-58] found that the shear capacity was influenced by the inelastic flexure deformation. This phenomenon is associated with the flexure-shear cracks widening and prevents the shear transformation in the concrete driven by aggregate interlocking. This leads to a so-called "shear-flexure interaction" [59]. To address the shear behavior together with the shear-flexure interaction effects, the development of rational models for assessing non-ductile RC structures is required and is a challenging task in structural engineering. In the past two decades, various frame element models have been developed to characterize the shear-flexure interaction in the non-ductile RC members [60-66]. Fiber section models with advanced analytical methodologies are among the models that are popular for use. For example, Marini and Spacone [60] employed the force-based fiber frame model to capture the shear-flexure interaction in RC columns. The shear and flexural mechanisms of their model [60] are coupled through the force-based formulation and Timoshenko beam theory at the element level. Although this model can represent the salient features of non-ductile RC columns, the shear constitutive must be calibrated on a case-by-case basis for each simulation. Martinelli [61] proposed the stiffness-based fiber element with the inclusion of the shear-flexure interaction for the analysis of the RC element subjected to cyclic loading. Ceresa et al. [62] used the MCFT to develop the displacement-based fiber beam element for the seismic analysis of the RC columns. The shear and flexure interacted at the fiber-section level via the MCFT principal as its model strategy. Feng and co-workers [63-64] used the multi-dimensional damage model to account for the shear-flexure interaction within the displacement-based fiber frame element for simulating the flexure-shear RC columns under cyclic loading. Although the models of Martinelli [61], Ceresa et al. [62], and Feng and co-workers [63-64] are of interest, their usage has been limited to computational expenses of practical usage due to several difficulties, such as high computational cost, complicated multi-dimensional constitutive relations, and high implementation effort. Subsequently, Sae-Long et al. [65-66] developed the displacement-based [65] and force-based [66] fiber frame models with the developed shear constitutive relations from Mergos and Kappos [67-68] to capture the shear-flexure interaction effects in the non-ductile RC columns. Their model's accuracy and performance are confirmed and validated through both experiments and numerical simulations. Furthermore, the model approach of Sae-Long et al. [65-66] is friendly to engineering practice due to the simplified model input parameters.

Up to date, the flexure-shear-interaction RC frame models on the foundation are rather limited. For example, Sae-Long et al. [69] applied the shear constitutive with the inclusion of the shear-flexure interaction effects of Sae-Long et al. [65-66] to present the displacement-based fiber frame model on the Winkler foundation for analysis of the non-ductile RC members on the foundation. Although this model is of interest, this foundation-frame model is limited only to the one-parameter foundation model (Winkler foundation). Therefore, based on the development path of the flexure-shear frame model on the foundation as above-mentioned, this paper aims to enrich the fiber frame element on the Kerr-type foundation with the inclusion of the shear-flexure interaction for the analysis of the non-ductile RC frame problems resting on the foundation. The proposed model is established based on the displacement-based formulation under the kinematic assumptions of the Timoshenko beam theory [70]. The uniaxial constitutive relations are employed to address the characteristics of the RC frame and foundation. The shear-flexure interaction effects are considered within the shear constitutive model as proposed by Sae-Long et al. [65-66]. All numerical procedures in this work are done on the general-purpose finite element platform FEAP [71]. Therefore, from the best knowledge of the authors, this is the first time to present the non-ductile RC frame model on the Kerr-type foundation with the inclusion of the shear-flexure interaction effects.

The directions for the presentation in this paper can be expressed as follows: In the first section, the governing differential equations of the proposed frame model on the Kerr-type foundation are introduced. It includes the equilibrium equations, compatibility equations, and force-deformation relations, respectively. Next, the displacement-based finite element formulation is presented. This approach is employed to derive the element stiffness matrix in this section. Subsequently, the shear model and its shear-flexure interaction procedures are presented. Then, two numerical simulations are provided to demonstrate the capability, accuracy, and efficiency of the proposed model. The first simulation examines the convergence studies, while the



second simulation is used to discuss the impact of the shear-flexure interaction effects on the responses of the proposed model. Finally, all the observations in this work are briefly concluded in the last section.

## 2. Governing Differential Equations of RC Frames on Kerr-Type Foundation

### 2.1 Equilibrium Equations

Based on the concept of the Kerr-type foundation model [37-38], the RC frame system on a foundation is modeled as the frame-foundation system as illustrated in Fig. 1. This system comprises the RC frame, the shear layer, and two layers of foundation springs. Thus, the equilibrium equations of this frame-foundation system can be obtained by considering the equilibrium of an infinitesimal segment  $dx$  of the frame and shear layer as follows.

The axial, bending, and transverse equilibriums of the RC frame are derived in a direct manner from the free body diagram of an infinitesimal segment  $dx$  of the frame, as shown in Fig. 2(a). These equilibrium equations can be expressed as:

$$\frac{dN(x)}{dx} = 0 \tag{1}$$

$$\frac{dM(x)}{dx} + V(x) = 0 \tag{2}$$

$$\frac{dV(x)}{dx} + w_y(x) - D_2(x) = 0 \tag{3}$$

where  $N(x)$ ,  $M(x)$ ,  $V(x)$  are the sectional axial force, bending moment, and shear force of the frame, respectively;  $w_y(x)$  is the transverse distributed load; and  $D_2(x)$  is the interactive force of an upper spring.

As similar to the RC frame part, the transverse equilibrium of the shear layer is obtained from the free body diagram of an infinitesimal segment  $dx$  of the shear layer, as shown in Fig. 2(b) as:

$$\frac{dV_s(x)}{dx} - D_1(x) + D_2(x) = 0 \tag{4}$$

where  $V_s(x)$  is the sectional shear force in the shear-layer; and  $D_1(x)$  is the interactive force of the lower spring.

The governing equilibrium equations of Eqs. (1)-(4) can be expressed in matrix form as:

$$\mathbf{L}_F^T \mathbf{D}_F(x) + \mathbf{L}_S^T \mathbf{D}_S(x) - \mathbf{P}(x) = 0 \tag{5}$$

where  $\mathbf{D}_F(x) = [N(x) \ M(x) \ V(x)]^T$  is the frame sectional force vector;  $\mathbf{D}_S(x) = [D_1(x) \ D_2(x) \ V_s(x)]^T$  is the foundation sectional force vector;  $\mathbf{P}(x) = [0 \ 0 \ w_y(x) \ 0]^T$  is the external load vector;  $\mathbf{L}_F$  and  $\mathbf{L}_S$  are the differential operators, which can be defined as:

$$\mathbf{L}_F = \begin{bmatrix} \frac{d}{dx} & 0 & 0 & 0 \\ 0 & \frac{d}{dx} & 0 & 0 \\ 0 & 1 & -\frac{d}{dx} & 0 \end{bmatrix} \text{ and } \mathbf{L}_S = \begin{bmatrix} 0 & 0 & 0 & 1 \\ 0 & 0 & 1 & -1 \\ 0 & 0 & 0 & -\frac{d}{dx} \end{bmatrix} \tag{6}$$

From the equilibrium equations in Eqs. (1)-(4), it can be inferred that this frame-foundation system is internally statically indeterminate when there are six internal forces but only four equilibrium equations are available. As a result, the internal forces cannot be determined from the equilibrium equations alone. However, this problem doesn't impact the displacement-based approach in this study since the internal forces are evaluated from the approximated displacements through the constitutive relations as discussed in the next section.

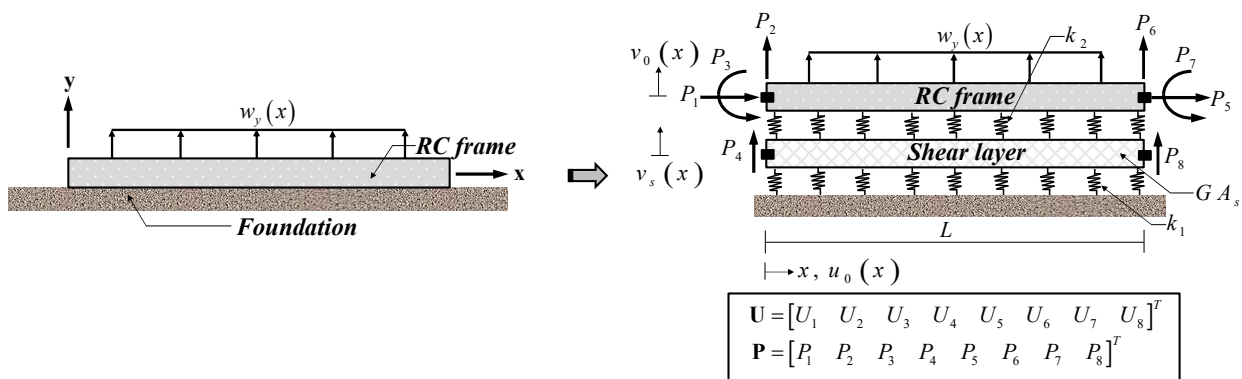


Fig. 1. Conceptual RC frame model on foundation.



2.2 Compatibility Equations

Based on the Timoshenko beam theory [70], the conjugate-work pairs of the internal forces for the RC frame as shown in the equilibrium equations (1)-(3) can be defined as:

$$\epsilon_0(x) = \frac{du_0(x)}{dx} \tag{7}$$

$$\kappa_0(x) = \frac{d\theta_0(x)}{dx} \tag{8}$$

$$\gamma_0(x) = \theta_0(x) - \frac{dv_0(x)}{dx} \tag{9}$$

where  $\epsilon_0(x)$  is the sectional axial strain that is the work conjugate of the sectional axial force  $N(x)$ ;  $\kappa_0(x)$  is the sectional bending curvature that is the work conjugate of the sectional bending moment  $M(x)$ ;  $\gamma_0(x)$  is the sectional shear strain that is the work conjugate of the sectional shear force  $V(x)$ ;  $u_0(x)$ ,  $\theta_0(x)$ , and  $v_0(x)$  are the displacement fields associated with the direction in axial, rotation, and transverse axis, respectively.

The compatibility equations of the Timoshenko frame in Eqs. (7)-(9) can be written in the matrix form as follows:

$$\mathbf{d}_F(x) = \mathbf{L}_F \mathbf{U}(x) \tag{10}$$

where  $\mathbf{d}_F(x) = [\epsilon_0(x) \ \kappa_0(x) \ \gamma_0(x)]^T$  is the frame sectional deformation vector; and  $\mathbf{U}(x) = [u_0(x) \ \theta_0(x) \ v_0(x) \ v_s(x)]^T$  is the displacement vector.

As presented by Limkatanyu et al. [38], the compatibility equations of the upper and lower foundation springs are obtained by considering the geometrical deformations of these foundation springs in Fig. 1. Thus, the compatibility relations of the lower and upper foundation springs are:

$$d_1(x) = v_s(x) \tag{11}$$

$$d_2(x) = v_0(x) - v_s(x) \tag{12}$$

where  $d_1(x)$  and  $d_2(x)$  are the foundation deformations of the lower and upper foundation springs, which are the work conjugate of the interactive forces  $D_1(x)$  and  $D_2(x)$ , respectively; and  $v_s(x)$  is the shear-layer displacement.

According to the intermediary shear layer of the Kerr-type foundation, they stem from the concept of the shear layer as proposed by Pasternak [33]. As suggested by Limkatanyu et al. [38], the compatibility equation of the shear layer can be written as:

$$\gamma_s(x) = -\frac{dv_s(x)}{dx} \tag{13}$$

where  $\gamma_s(x)$  is the shear strain of the shear layer.

The compatibility relations of the foundation in Eqs. (11)-(13) can be expressed in the matrix form as:

$$\mathbf{d}_s(x) = \mathbf{L}_s \mathbf{U}(x) \tag{14}$$

It is noteworthy to emphasize that the system equilibriums relate to the system compatibilities through the differential operators. This leads to a contragradient nature in the RC frame model on the Kerr-type foundation for this study.

2.3 Force-Deformation Relations

For the nonlinear constitutive relations to address the behavior of the RC frame on foundation, this study employs the uniaxial constitutive laws to represent the characteristics of each material, namely the Kent and Park concrete model [72], the Menegotto and Pinto steel model [73], the shear model as proposed by Sae-Long et al. [65-66], and the linear foundation models of Limkatanyu et al. [26] to represent the upper and lower foundation springs and shear layer. These constitutive relations are demonstrated in Fig. 3. Thus, the nonlinear force-deformation relations can be written as:

$$\mathbf{D}_F(x) = \Phi[\mathbf{d}_F(x)] \tag{15}$$

$$\mathbf{D}_s(x) = \Omega[\mathbf{d}_s(x)] \tag{16}$$

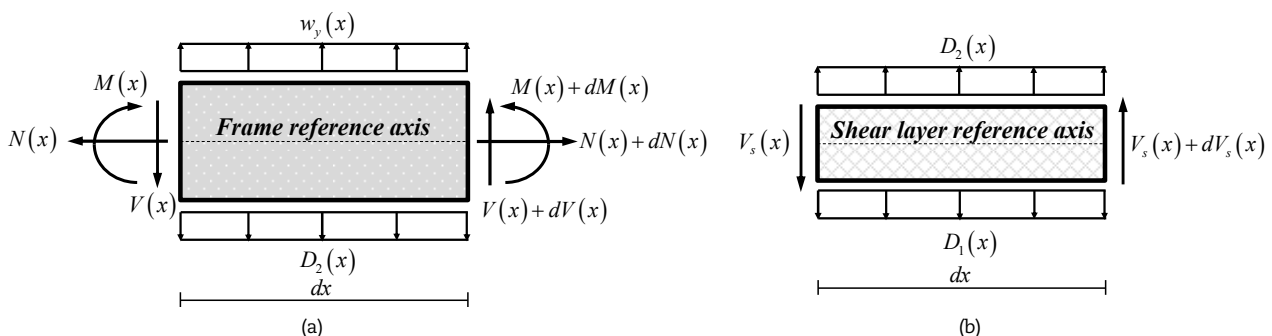


Fig. 2. Free body diagrams: (a) frame; and (b) shear layer.



The incremental form of the nonlinear force-deformation relations in Eqs. (15) and (16) for the frame model on the Kerr-type foundation can be written by linearization as:

$$D_F(x) = D_F^0(x) + k_F^0(x) \Delta d_F(x) \tag{17}$$

$$D_S(x) = D_S^0(x) + k_S^0(x) \Delta d_S(x) \tag{18}$$

where superscript 0 on the variables denotes the initial value during the iterative procedures;  $k_F^0(x)$  and  $k_S^0(x)$  are the sectional stiffness of the RC frame and foundation, respectively.

In this study, the fiber-section model of Spacone and Limkatantu [74] was employed to refine the frame cross-section into a discrete fiber for analysis, as shown in Fig. 4. Based on this approach and the Timoshenko beam theory, the axial and bending mechanisms naturally interact at the sectional level. As a result, the axial force and bending moment are calculated from the summation of the normal stress in each fiber as follows:

$$N(x) = \sum_{r=1}^{r=nfib} \sigma_r A_r \tag{19}$$

$$M(x) = - \sum_{r=1}^{r=nfib} y_r \sigma_r A_r \tag{20}$$

where  $\sigma_r$ ,  $A_r$ , and  $y_r$  are the normal stress, section area, and distance measured from the reference axis of the  $r^{th}$  fiber in the cross section;  $r$  is a generic fiber; and  $nfib$  is total fiber count.

Based on the discrete forms in Eqs. (19) and (20), the frame sectional force vector  $D_F(x)$  can be rewritten as follows:

$$D_F(x) = \left[ \sum_{r=1}^{r=nfib} \sigma_r A_r \quad - \sum_{r=1}^{r=nfib} y_r \sigma_r A_r \quad V(x) \right]^T \tag{21}$$

It is interesting to observe from Eq. (21) that the axial and bending mechanisms are dependent on the discrete sections, while the shear mechanism is independent of the fiber-section model [74]. In other words, the shear responses can be modeled with only one fiber section, as demonstrated by Sae-Long et al. [65-66].

As suggested by Spacone and Limkatantu [74], sectional stiffness  $k_F^0(x)$  and  $k_S^0(x)$  can be defined through the fiber-section model [74] and the Kerr-type foundation model [38] as follows:

$$k_F(x) = \begin{bmatrix} \sum_{r=1}^{r=nfib} E_r A_r & - \sum_{r=1}^{r=nfib} y_r E_r A_r & 0 \\ - \sum_{r=1}^{r=nfib} y_r E_r A_r & \sum_{r=1}^{r=nfib} y_r^2 E_r A_r & 0 \\ 0 & 0 & GA(x) \end{bmatrix} \tag{22}$$

$$k_S(x) = \begin{bmatrix} k_1(x) & 0 & 0 \\ 0 & k_2(x) & 0 \\ 0 & 0 & GA_s(x) \end{bmatrix} \tag{23}$$

where  $E_r$  is the elastic modulus of the  $r^{th}$  fiber;  $GA(x)$  is the sectional shear stiffness of the RC frame;  $GA_s(x)$  is the sectional shear stiffness of the shear layer; and  $k_1(x)$  and  $k_2(x)$  are the foundation spring stiffnesses of the lower and upper spring layers, respectively.

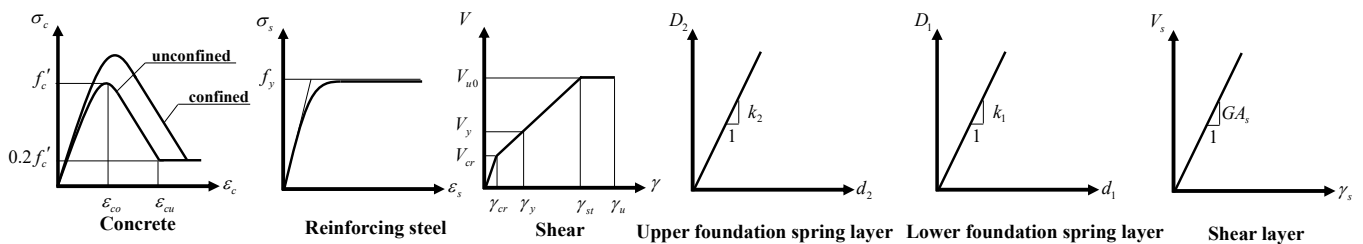


Fig. 3. Uniaxial material constitutive relations.



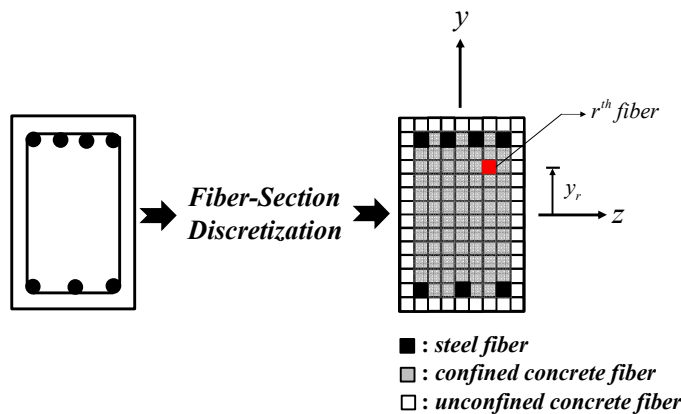


Fig. 4. Fiber-section model for the RC frame cross section [74].

### 3. Displacement-Based Formulation: Finite Element Formulation

In the displacement-based formulation, the displacement fields are treated as a primary variable, while the sectional forces are assumed as a secondary variable that can be evaluated from the displacement fields through the force-deformation relations. As a result, the compatibility equations (7)-(14) are satisfied in the strong sense, while the equilibrium equations (1)-(5) are satisfied in the integral sense. The weighted residual form of the equilibrium overall in the distance domain [0, L] can be expressed as follows:

$$\int_L \delta \mathbf{U}^T(x) [\mathbf{L}_F^T \mathbf{D}_F(x) + \mathbf{L}_S^T \mathbf{D}_S(x) - \mathbf{P}(x)] dx = 0 \tag{24}$$

where  $L$  is the length of RC frame; and  $\delta \mathbf{U}$  is a statically admissible virtual section displacement vector.

Imposing the force-deformation relations of Eqs. (17) and (18), compatibility equations of Eqs. (10) and (14) into Eq. (24) and subsequently applying integration by parts, the equation (24) yields:

$$\int_L \begin{Bmatrix} \mathbf{L}_F \delta \mathbf{U}(x) \\ \mathbf{L}_S \delta \mathbf{U}(x) \end{Bmatrix}^T \begin{bmatrix} \mathbf{k}_F^0(x) & 0 \\ 0 & \mathbf{k}_S^0(x) \end{bmatrix} \begin{Bmatrix} \mathbf{L}_F \Delta \mathbf{U}(x) \\ \mathbf{L}_S \Delta \mathbf{U}(x) \end{Bmatrix} dx = \int_L \delta \mathbf{U}^T(x) \mathbf{P}(x) dx + \delta \mathbf{U}^T \mathbf{P} - \int_L \mathbf{L}_F^T \delta \mathbf{U}^T(x) \mathbf{D}_F^0(x) dx - \int_L \mathbf{L}_S^T \delta \mathbf{U}^T(x) \mathbf{D}_S^0(x) dx \tag{25}$$

where  $\mathbf{P}$  is the nodal force vector, which corresponds with the nodal displacement vector  $\mathbf{U}$ , as illustrated in Fig. 1.

Based on the displacement-based formulation, the displacement fields are evaluated from the nodal displacement  $\mathbf{U}$  through the displacement shape functions  $\mathbf{N}_{FS}(x)$  as follows:

$$\mathbf{U}(x) = \mathbf{N}_{FS}(x) \mathbf{U} \tag{26}$$

Employing the relation in Eq. (26) and accounting for the arbitrariness of  $\delta \mathbf{U}$ , the relation in Eq. (25) leads to the element stiffness equation as:

$$(\mathbf{K}_F + \mathbf{K}_S) \Delta \mathbf{U} = \mathbf{P} + \mathbf{P}_{ext} - (\mathbf{P}_F^0 + \mathbf{P}_S^0) \tag{27}$$

where  $\mathbf{K}_F = \int_L \mathbf{B}_F^T(x) \mathbf{k}_B(x) \mathbf{B}_F(x) dx$  is the frame element stiffness matrix;  $\mathbf{K}_S = \int_L \mathbf{B}_S^T(x) \mathbf{k}_S(x) \mathbf{B}_S(x) dx$  is the Kerr-type foundation element stiffness matrix;  $\mathbf{P}_{ext} = \int_L \mathbf{N}_{FS}^T(x) \mathbf{P}(x) dx$  is the equivalent load vector due to the external load  $w_y(x)$ ;  $\mathbf{P}_F^0 = \int_L \mathbf{B}_F^T(x) \mathbf{D}_F^0(x) dx$  is the resistant force vector of the RC frame;  $\mathbf{P}_S^0 = \int_L \mathbf{B}_S^T(x) \mathbf{D}_S^0(x) dx$  is the resistant force vector of the Kerr-type foundation;  $\mathbf{B}_F(x)$  and  $\mathbf{B}_S(x)$  are the deformation-displacement matrices.

It is noted that the displacement shape functions  $\mathbf{N}_{FS}(x)$  of Eq. (26) must be selected with care when the shear-locking phenomenon may occur [75]. This incident leads to the unrealistic prediction of the shear responses in the structural models as reported in the literature [76-78]. For this study, the so-called “linked displacement shape functions” as proposed by Sae-Long et al. [65] are employed to overcome the shear-locking phenomenon. These interpolation functions are established based on the slender beam conditions with one higher degree of interpolation function for the transverse displacement when compared to the interpolation function of the rotation field. Therefore, the linked displacement shape functions can be expressed as [65]:

$$\mathbf{N}_{FS}(x) = \begin{bmatrix} 1 - \frac{x}{L} & 0 & 0 & 0 & \frac{x}{L} & 0 & 0 & 0 \\ 0 & 0 & 1 - \frac{x}{L} & 0 & 0 & 0 & \frac{x}{L} & 0 \\ 0 & 1 - \frac{x}{L} & \frac{x}{2} - \frac{x^2}{2L} & 0 & 0 & \frac{x}{L} & -\frac{x}{2} + \frac{x^2}{2L} & 0 \\ 0 & 0 & 0 & 1 - \frac{x}{L} & 0 & 0 & 0 & \frac{x}{L} \end{bmatrix} \tag{28}$$

With the differential operators  $\mathbf{L}_F$  and  $\mathbf{L}_S$ , the deformation-displacement matrices  $\mathbf{B}_F(x)$  and  $\mathbf{B}_S(x)$  can be expressed as follows:



$$\mathbf{B}_F(x) = \mathbf{L}_F \mathbf{N}_{FS}(x) = \begin{bmatrix} -\frac{1}{L} & 0 & 0 & 0 & \frac{1}{L} & 0 & 0 & 0 \\ 0 & 0 & -\frac{1}{L} & 0 & 0 & 0 & \frac{1}{L} & 0 \\ 0 & \frac{1}{L} & \frac{1}{2} & 0 & 0 & -\frac{1}{L} & \frac{1}{2} & 0 \end{bmatrix} \tag{29}$$

$$\mathbf{B}_S(x) = \mathbf{L}_S \mathbf{N}_{FS}(x) = \begin{bmatrix} 0 & 0 & 0 & 1 - \frac{x}{L} & 0 & 0 & 0 & \frac{x}{L} \\ 0 & 1 - \frac{x}{L} & \frac{x}{2} - \frac{x^2}{2L} & -1 + \frac{x}{L} & 0 & \frac{x}{L} & -\frac{x}{2} + \frac{x^2}{2L} & -\frac{x}{L} \\ 0 & 0 & 0 & \frac{1}{L} & 0 & 0 & 0 & -\frac{1}{L} \end{bmatrix} \tag{30}$$

### 4. Shear Model

To elucidate the shear mechanism and its interaction effects within the proposed frame-foundation model, this study employs the shear model as proposed by Sae-Long et al. [65-66]. This shear model was developed from the shear constitutive relations of Mergos and Kappos [67-68] together with the UCSD (University of California, San Diego) shear-strength model of Priestley et al. [79]. Therefore, this model can account for the degradation of the shear strength due to the influence of the inelastic flexure deformation as found in the experiments and simulations [44, 45, 55-58].

At the outset, the relationship between shear force and shear strain starts from the undamaged primary curve as shown in Fig. 5. This diagram comprises four intervals but only three linear slopes. The first interval (with linear OA) presents the behavior of the RC frame section before cracking. The shear force  $V_{cr}$  and shear strain  $\gamma_{cr}$  at the onset of the concrete cracking at point A can be evaluated as suggested by Sezen and Moehle [57] as:

$$V_{cr} = \left( \frac{f_{tensile}}{a/h} \sqrt{1 + \frac{N}{f_{tensile} A_g}} \right) 0.80 A_g \tag{31}$$

$$\gamma_{cr} = \frac{V_{cr}}{(GA)_0} \tag{32}$$

where  $f_{tensile}$  is the nominal tensile strength in concrete;  $a/h$  is shear span ratio;  $N$  is the compressive load;  $A_g$  is gross cross sectional area; and  $(GA)_0 = 0.80GA_g$  is the undamaged shear stiffness.

The second interval (with linear AB) represents the post-cracking section for the RC frame cross-section, while the third interval (with linear BC) characterizes the RC frame cross-section after the onset of the flexural yielding. The shear force  $V_y$  and shear strain  $\gamma_y$  at the onset of the flexural yielding at point B are naturally detected by the fiber-section model when the sectional axial strain reaches the yield strain of the longitudinal reinforcement. Both the values of the shear force and shear strain in this stage are kept at their shear force  $V_y$  and shear strain  $\gamma_y$ . Next, the shear force at the onset of the transverse reinforcement yielding at point C can be computed based on the UCSD shear-strength model of Priestley et al. [79] as:

$$V_u = \overbrace{k_p \sqrt{f'_c} (0.8A_g)}^{\text{Concrete component}} + \overbrace{\frac{A_v f_{yv} D'}{s} \cot 30^\circ}_{\text{Truss component}} + \overbrace{N \tan \beta}_{\text{Arch component}} \tag{33}$$

where  $V_u$  is the ultimate shear force;  $k_p$  is the factor associated with the sectional curvature ductility demand  $\mu_\varphi$  as shown in Fig. 6;  $f'_c$  is the concrete compressive strength in the cylinder specimens;  $s$ ,  $A_v$ , and  $f_{yv}$  are the spacing, area, and yield stress of the transverse reinforcement;  $D'$  is the distance measured parallel to the applied shear between the centers of the longitudinal reinforcement; and  $\beta$  is the angle between the column axis and the line connecting the centers of the flexural compression zones at the top and bottom of the column ends. The value of  $V_{u0}$  in the undamaged primary curve in Fig. 5 is simply determined from the UCSD shear-strength model in Eq. (33) by setting the sectional curvature ductility demand lower than 3.

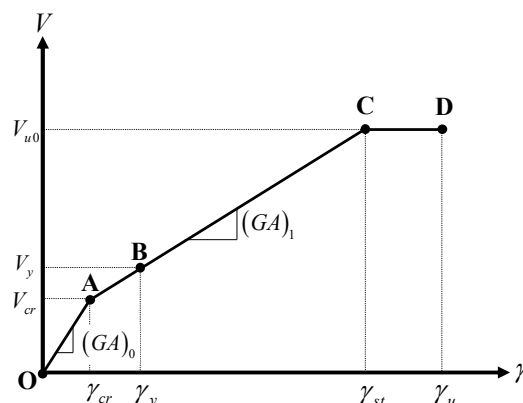


Fig. 5. Undamaged primary curve of the shear model [65].



As suggested by Mergos and Koppas [68], the shear strain  $\gamma_{st}$  at the onset of the transverse reinforcement yielding can be evaluated as follows:

$$\gamma_{st} = \Phi_1 \Phi_2 \gamma_{truss} \tag{34}$$

where  $\Phi_1 = 1 - 1.07(N / f_c' A_g)$  is the corrected parameter associated with the axial force;  $\Phi_2 = 5.37 - 1.59 \min(2.5, a / h)$  is the corrected parameter associated with the aspect ratio; and  $\gamma_{truss}$  is the shear strain at the onset of the transverse reinforcement as computed by using the truss analogy approach [80]. The shear strain  $\gamma_{truss}$  is defined as:

$$\gamma_{truss} = \frac{V_{cr}}{(GA)_0} + \frac{A_v f_{yv}}{s E_s b \rho_w \sin^4 \omega \cot \omega} \left( \sin^4 \omega + \frac{E_s}{E_c} \rho_w \right) \tag{35}$$

where  $E_c$  is the concrete elastic modulus;  $E_s$  is the reinforcement steel elastic modulus;  $\rho_w$  is the volumetric ratio;  $b$  is the sectional width; and  $\omega$  is the angle between the reference axis and the line of diagonal struts. In this work, the optimal value of the angle  $\omega$  follows that suggested by Mergos and Koppas [68] of  $\omega = 45^\circ$ .

The last interval (with linear CD) addresses the behavior of the RC frame cross-section after the onset of the transverse reinforcement yielding. Based on the regression analysis of RC shear-critical columns from the work of Mergos and Koppas [68], the shear strain  $\gamma_u$  at the onset of the shear failure can be determined as follows:

$$\gamma_u = \Psi_1 \Psi_2 \Psi_3 \gamma_{st} \geq \gamma_{st} \tag{36}$$

where  $\Psi_1 = 1 - 2.5 \min(0.4, N / f_c' A_g)$  is the modification factor associated with the axial-load effect;  $\Psi_2 = \min(6.25, a^2 / h^2)$  is the modification factor associated with the aspect ratio; and  $\Psi_3 = 0.31 + 17.8 \min(A_v f_{yv} / bs f_c', 0.08)$  is the modification factor associated with the amount of transverse reinforcement.

Based on the influence of the inelastic flexural deformation as demonstrated in the UCSD shear-strength model [79], the shear force-shear strain relation in Fig. 5 will depart from the undamaged primary curve into the damaged envelope curve, as shown in Fig. 7. This reduced phenomenon is called “shear-flexure interaction effects”, which are found in the RC flexure-shear critical members [55-69]. These effects lead to the degradation of shear strength and shear stiffness in the concrete sections [65, 79]. Therefore, a special procedure to account for these effects within the proposed model is required in the finite implementation when the sectional shear force and shear stiffness are unknown variables. This study uses the so-called “modified shear-flexure interaction procedures” as proposed by Sae-Long et al. [65-66] to evaluate both the sectional shear force and shear stiffness within the plastic hinge zone. This approach was modified from the framework of the shear-flexure interaction procedures of Mergos and Koppas [68] based on the reference shear stiffness  $GA_{ref}$ . A step-by-step procedure to calculate the sectional shear force and shear stiffness in the plastic hinge zone is presented in Fig. 8. More details of the approach are discussed in the work of Sae-Long et al. [65-66].

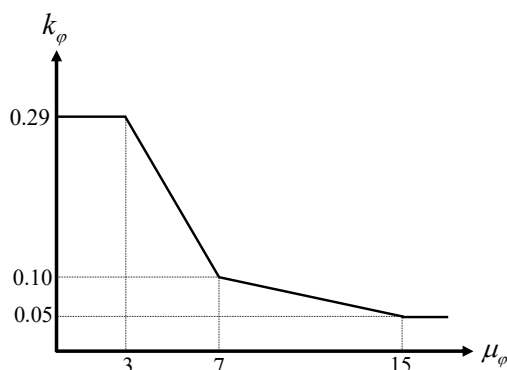


Fig. 6. Relation between the factor  $k_\varphi$  and curvature ductility demand  $\mu_\varphi$  [68].

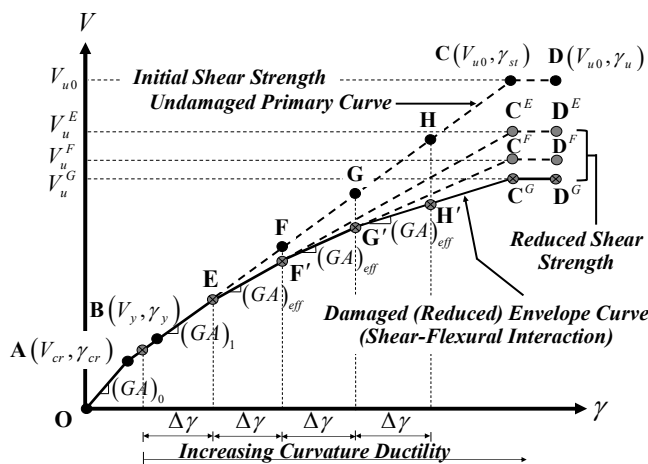


Fig. 7. Damaged envelope curve of the shear model [65-66].



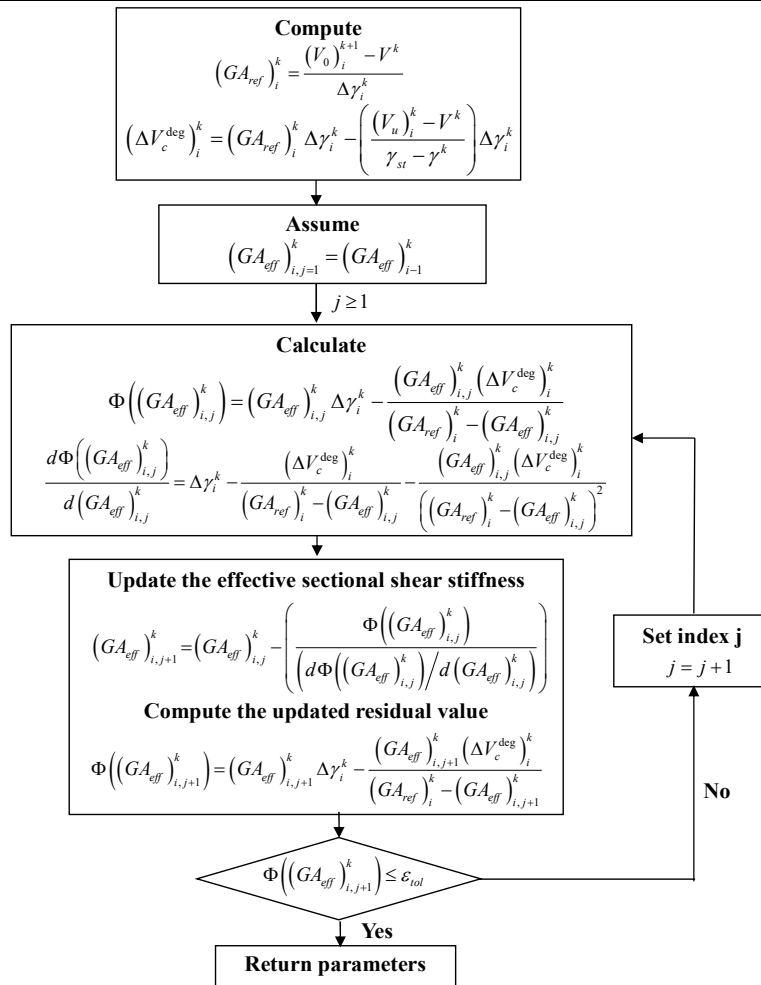


Fig. 8. A-step-by-step to evaluate the sectional shear force and shear stiffness [65].

### 5. Numerical Simulations

To verify the capability, accuracy, and efficiency of the proposed frame-foundation model, two numerical simulations are employed in this work. The first simulation is the convergence studies, which investigates the accuracy and efficiency of the proposed frame-foundation model. The second simulation discusses the impact of the shear-flexure interaction effects on the responses of the non-ductile RC frame model on the foundation models. Both simulations employ the RC flexure-shear critical column, which fails in shear after the onset of the flexural yielding, to assess the achievement of the proposed model. Furthermore, the shear constitutive model of two non-ductile columns, as discussed in Section 4, was verified and well accepted among the experiments and simulations [65, 66, 81, 82].

#### 5.1 Numerical Simulation I: Convergence Studies

A simply supported RC frame on an infinitely long Kerr-type foundation subjected to a constant compressive load of 667 kN at both end boundaries and subjected to a concentrated load at midspan under displacement control is illustrated in Fig. 9. This frame-foundation system is employed in this simulation to assess the convergence trend and to investigate the amount of the proposed element to reach the benchmark responses. The material properties, geometric, and reinforcement details of the RC frame come from the column specimens labeled column 2CLD12 as conducted by Sezen [81] as shown in Fig. 9. The Kerr-type foundation properties come from the work of Antonio et al. [83], based on the soil properties of Shiri [84]. The upper and lower springs are considered linear elastic springs with the stiffness of  $k_2 = 3.56 \times 10^3 \text{ kN/m}^2$  and  $k_1 = 5.086 \times 10^2 \text{ kN/m}^2$ , respectively. The shear layer is also defined by linear elasticity with the stiffness of  $GA_s = 3.324 \times 10^2 \text{ kN}$ . To account for the influence of the infinitely extended foundation, Alemdar and Gülkan [85] suggested replacing this infinitely long distance with a vertical spring with stiffness  $k_{end} = \sqrt{k_1 GA_s}$  at both boundary ends of the RC frame. Due to the symmetry property, only half of the frame-foundation system is employed to analyze, as illustrated in Fig. 9. It needs to be emphasized that each proposed element employs seven Gauss-Lobatto integration points and forty fibers to present all the responses in this simulation. This amount is sufficient to represent both global and local responses of the displacement-based structure models as confirmed in the literature [22, 26, 65, 69].

Figure 10(a) presents the convergence studies to gain the converged global response (midspan load-deflection response  $P - \delta$ ). The result shows that sixteen proposed elements are sufficient to reach the benchmark response established with a mesh consisting of thirty-two proposed elements. The load-displacement response yield already satisfies the benchmark response with a mesh of eight proposed elements. However, the shear failure cannot be detected by this number of elements due to the insufficiently refined mesh to capture the sectional inelastic flexural deformation as reported by Sae-Long et al. [69]. There are two circumstances in the global response. At the deflection  $\delta = 6.12 \text{ mm}$ , the first plastic hinge forms at the midspan due to the load and restraint conditions. During the displacement control, the shear failure is detected at the deflection  $\delta = 10.3 \text{ mm}$ .



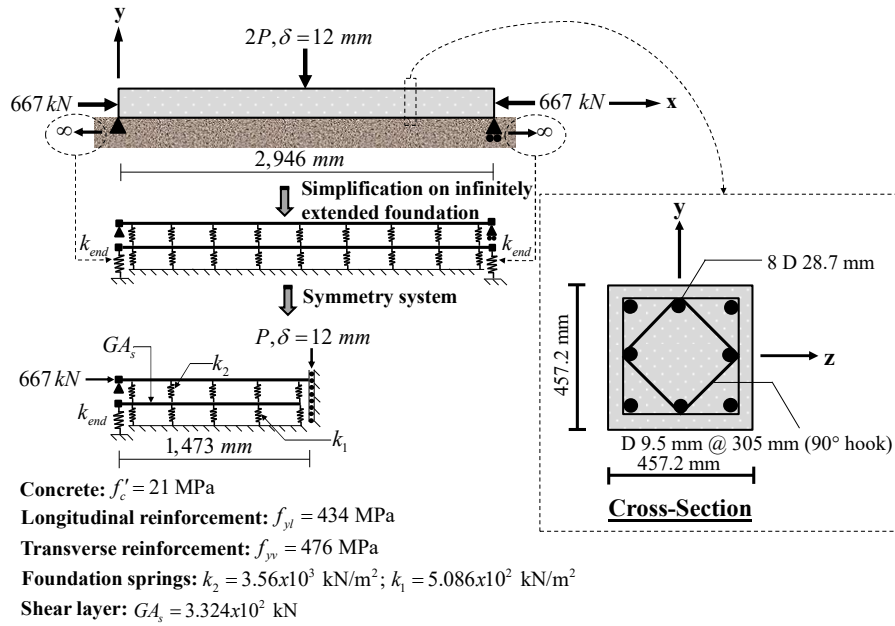


Fig. 9. Numerical simulation I: Convergence studies.

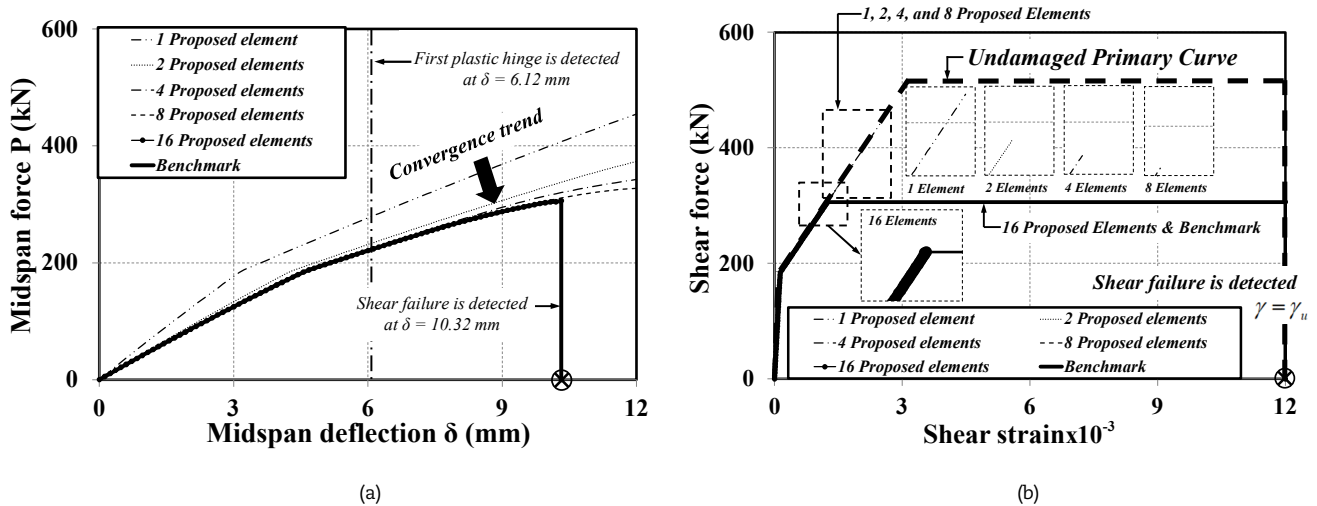


Fig. 10. Response of numerical simulation I at midspan position: (a) global response; and (b) local response.

Figure 10(b) shows the convergence studies used to obtain the converged local response (shear force-shear strain relationship at the midspan). As seen in the global response in Fig. 10(a), a mesh of 16 proposed elements is sufficient to achieve the benchmark response represented by a mesh of 32 proposed elements. Furthermore, this diagram shows that the shear failure requires a sufficiently refined mesh for the prediction of the sectional curvature ductility demand within the inelastic zone. A mesh containing 1, 2, 4, and 8 proposed elements demonstrates insufficient accuracy to capture the inelastic flexural responses. Therefore, these amounts cannot capture the shear failure and shear-flexure interaction effects within the non-ductile RC members. Following the shear model with sixteen proposed elements, the first plastic hinge rotation forms at the shear strain  $\gamma_y = 5.2271 \times 10^{-4}$ , corresponding with the deflection of  $\delta = 6.12 \text{ mm}$ . When the sectional curvature ductility demand reaches its threshold value of 3, the shear-flexure interaction is activated, resulting in the degradation of the sectional shear stiffness and an increase in shear strain. Shear failure is captured when the shear strain reaches its threshold ultimate value  $\gamma_u = 1.2 \times 10^{-2}$ . This failure value matches the observation from the experiment of this column as proposed by Mergos and Kappos [67-68].

From the convergence studies in this simulation, it can be concluded that the number of used elements is necessary to capture the shear-flexure interaction within the inelastic flexure zone. For the frame-foundation model in this study, a mesh containing 16 proposed elements is the minimum requirement for using the analysis of the non-ductile RC frame on the Kerr-type foundation both at the global and local levels.

5.2 Simulation II: Impacts of the shear-flexure interaction on the responses of the frame on foundation models

To examine the impacts of the shear-flexure interaction on both the global and local responses of the proposed model, the simply supported RC frame on an infinitely long Kerr-type foundation in Fig. 11 is employed in this simulation. The frame is subjected to a constant axial load at the ends of the structure and subjected to a concentrated load under the displacement control at midspan. As shown in Fig. 11, the material properties, geometric, and reinforcement details of the column labeled 2CMH18 as conducted by Lynn [82] are used to characterize the behaviors of the non-ductile RC frame in this study. The material properties of the Kerr-type foundation follow those employed by Morfidis [86]. The upper foundation spring layer is modeled with



linear elastic springs with a stiffness of  $k_2 = 1.63 \times 10^4 \text{ kN/m}^2$ , while the lower foundation spring layer exhibits linear elasticity with a stiffness of  $k_1 = 2.33 \times 10^3 \text{ kN/m}^2$ . The shear layer is prescribed in the linear elastic layer with a constant stiffness of  $GA_s = 2.991 \times 10^4 \text{ kN}$ . Due to the symmetry property, only half of the frame-foundation system is used to analyze, while the influence of the infinitely long foundation is represented by the vertical springs with stiffness  $k_{end} = \sqrt{k_1 GA_s}$  at both boundary ends of the RC frame, as illustrated in Fig. 11. To clearly demonstrate the impact of the shear-flexure interaction effects on the frame's responses, three numerical frame-foundation models are used, namely (a) the proposed frame model on the Kerr-type foundation; (b) the classical frame model on the Kerr-type foundation; and (c) the classical frame model on the Winkler foundation. It is worthwhile to note that the so-called "classical" frame models are the frame models without accounting for the effects of the shear-flexure interaction. Based on the convergence studies in the previous simulation, a mesh of sixteen proposed elements with seven Gauss-Lobatto integration points and forty fibers is employed to represent the characteristics of this non-ductile RC frame on the foundation in this simulation.

Figure 12(a) presents the load-deflection at the midspan obtained from the three numerical frame-foundation models. This diagram clearly demonstrates that the effect of the shear-layer leads to the stiffening element stiffness as observed from a series of the frame models on the Kerr-type foundation when compared to the frame on the Winkler foundation. The initial stiffness of the frame models on the Kerr-type foundation is higher than the initial stiffness of the Winkler-based frame model by about 3.49% on average. During the applied displacement control, all numerical frame-foundation models capture the first plastic rotation at point A with a deflection of  $\delta = 5.10 \text{ mm}$ . Finally, the shear failure is detected by only the proposed model at a deflection of  $\delta = 12.15 \text{ mm}$ , while a series of classical frame-foundation models cannot capture this failure characteristic. This proves the capability of the proposed frame-foundation model to overcome the series of classical frame-foundation models.

Figure 12(b) illustrates the relationship between shear force and shear strain at the midspan. Due to the load and boundary conditions, this location fails in shear due to the influence of the shear-flexure interaction as governed by the shear constitutive law in Section 4 for the proposed model. When the shear-flexure interaction is activated with the increase in the sectional curvature ductility demand, the shear strength and shear stiffness are reduced, resulting in a rapid increase in the shear strain. During the applied load, the first plastic hinge rotation is detected at the shear strain of  $\gamma_y = 1.24 \times 10^{-4}$  for the series of frame models on the Kerr-type foundation, while the frame model on the Winkler foundation predicts this occurrence at the shear strain of  $\gamma_y = 1.19 \times 10^{-4}$ . This difference is caused by the shear-layer and additional foundation spring layer in the Kerr-type foundation, resulting in stiffened system stiffness. Finally, shear failure occurs in the proposed frame model when the shear strain reaches its ultimate value of  $\gamma_u = 4.6 \times 10^{-3}$ , as predicted from Eq. (36). This value corresponds well with the experiment and simulations as suggested by Mergos and Kappos [68]. Conversely, the series of classical frame-foundation models cannot exhibit this failure behavior due to the lack of accounting for the shear-flexure interaction effects. Therefore, the shear responses of these models also follow the shear primary curve as shown in Fig. 5.

Figure 13 shows the relationship between the shear force and curvature ductility demand at the midspan. The shear failure envelope (bold dash line) is established from the UCSD shear-strength model of Priestley et al. [79] in Eq. (33) and is used to detect the shear failure. The result shows that the shear-flexure interaction effects play an important role in analyzing the non-ductile RC members. It can be seen in this diagram that this frame would not have failed in shear if the shear-flexure interaction had not been considered as clearly observed from the proposed model when compared to the classical frame model on the Kerr-type foundation. Shear failure occurs when the shear force meets the shear failure envelope at the curvature ductility demand of  $\mu_\phi = 6.8$  for the proposed model. As similarly observed in the shear force-shear strain relation in Fig. 12(b), the shear layer and additional foundation spring layer in the Kerr-type foundation lead to the stiffening system stiffness, resulting in a higher shear force resistance when compared to the frame model on the Winkler foundation.

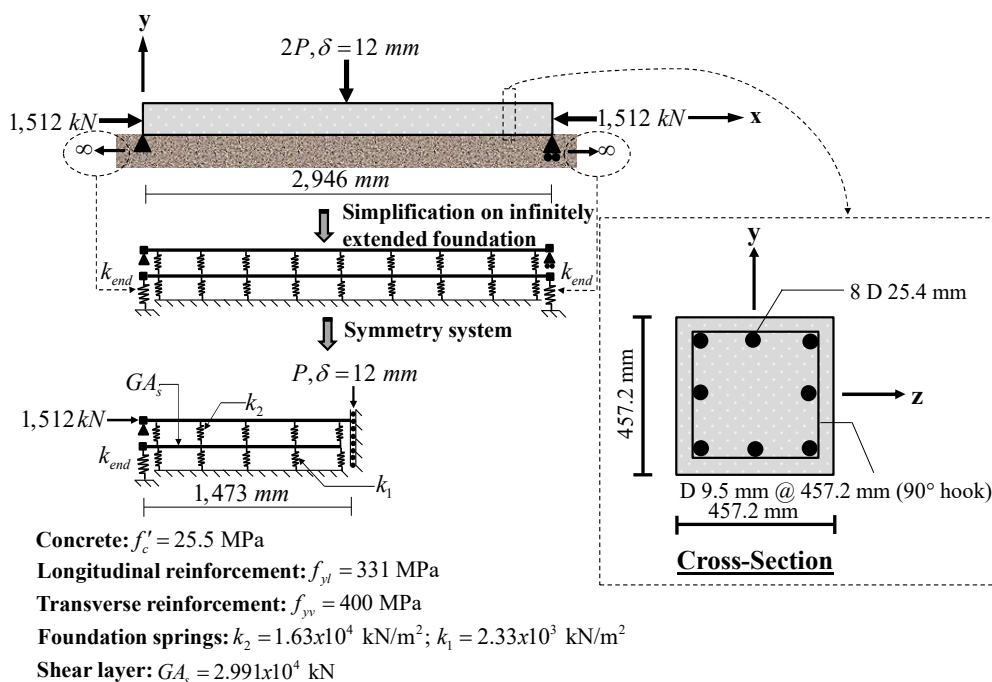


Fig. 11. Numerical simulation II: Impact of the shear-flexure interaction and structure-foundation interaction on the responses.



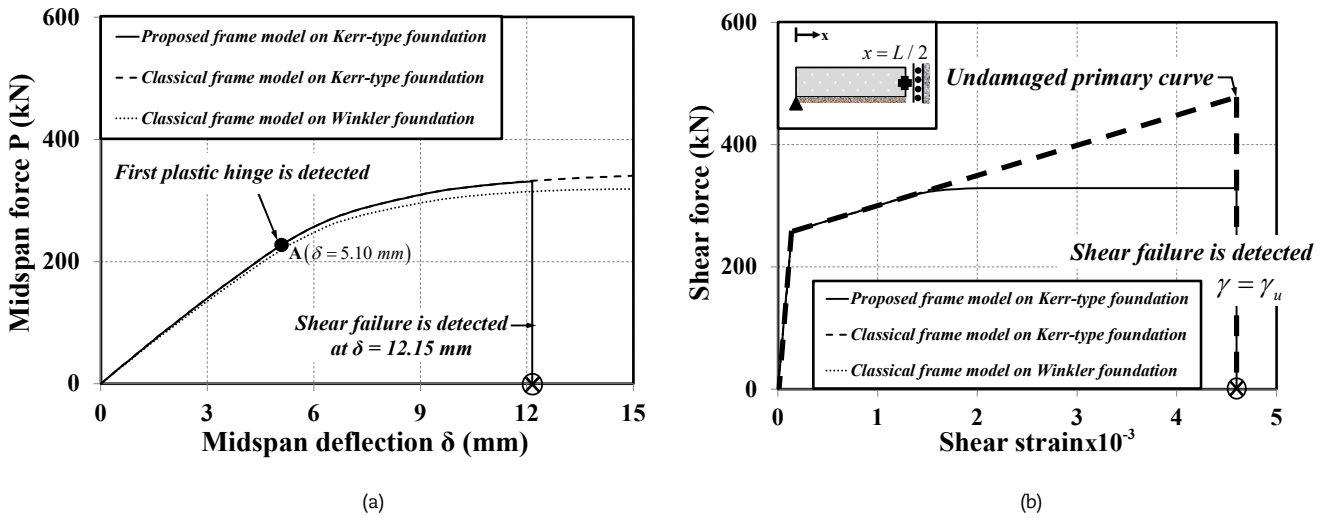


Fig. 12. Response of numerical simulation II at midspan position: (a) global response; and (b) local response.

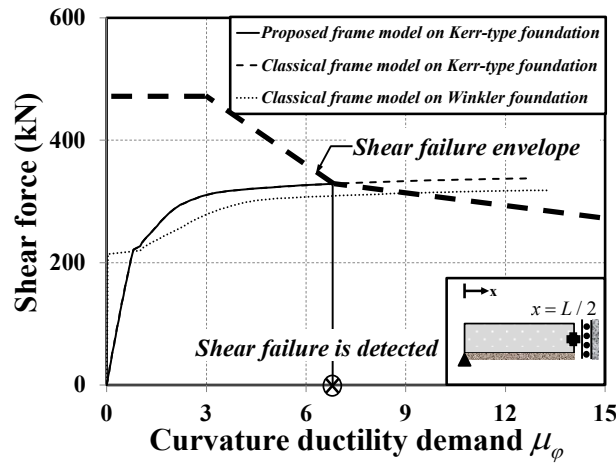


Fig. 13. Shear force – curvature ductility demand relation of numerical simulation II at midspan position.

From this simulation, it can be concluded that the influence of the shear-flexure interaction plays an essential role in the prediction of the shear failure due to the impact of the inelastic flexural deformation. These effects lead to the degradation of the shear strength and shear stiffness, resulting in the weakened system stiffness, while the influence of the shear-layer and additional foundation spring layer of the Kerr-type foundation makes the element stiffness increase when compared to the responses of the Winkler-based frame model. Therefore, these interaction effects are crucial for the analysis of non-ductile RC members resting on the foundation.

### 6. Conclusion

This paper presents the shear-flexure-interaction frame model on the Kerr-type foundation for analysis of non-ductile RC members resting on the foundation. The proposed model is formulated based on the displacement-based finite element formulation together with the hypothesis of Timoshenko beam theory. The uniaxial constitutive laws are employed to represent the characteristics of the RC frame and foundation. The shear-flexure interaction effects are taken into account for the proposed model within the shear constitutive model as proposed by Sae-Long et al. [65-66]. The modified Mergos and Kappos interaction procedure, as proposed by Sae-Long et al. [65], is employed to predict the sectional shear force and shear stiffness within the inelastic flexural zone. To verify the capability, accuracy, and efficiency of the proposed model, two flexure-shear critical columns on the foundation are employed in this work. From the analytical results, it can be concluded as follows:

The first simulation presents the accuracy and efficiency of the proposed model through parametric studies. The parametric results confirm that a mesh size of 16 proposed elements is sufficient to represent the converged responses at both global and local levels. It needs to be emphasized that although the mesh size of 8 proposed elements is already ample to get the converged maximum load, this amount is insufficient to predict the sectional curvature ductility demand in the inelastic zone. As a result, the mesh containing 1, 2, 4, and 8 elements cannot capture the shear failure within the non-ductile RC frame on the foundation.

The second simulation discusses the importance of the shear-flexure interaction for the analysis of the non-ductile RC frame on the foundation and confirms the capability of the proposed model to capture the behavior of shear failure when compared to the classical frame-foundation models. The shear-flexure interaction leads to the degradation of the shear strength and shear stiffness within the plastic hinge zone, resulting in an instant increase in the sectional shear strain. Furthermore, the shear layer and additional foundation spring layer of the Kerr-type foundation enhance the system stiffness to be stiffened as obviously demonstrated when compared to the Winkler-based frame model. As a result, the shear-flexure interaction and foundation-structure interaction are critical in the analysis of the non-ductile members resting on foundation.



The next step in this work is to develop and extend the shear constitutive model for the prediction of the non-ductile RC member's behaviors associated with the axial loss capacity. This concept can be applied within the full nonlinear static and dynamic analyses of non-ductile RC structures. Therefore, we hope that the next work will be interesting and have benefits for the research community in the future.

### Author Contributions

S. Limkatanyu played a role in deriving the formulation, interpreting the numerical results and partially writing the manuscript; W. Sae-Long played a role in deriving the formulation, implementing the numerical model, interpreting the numerical results, and writing main parts of the manuscript; N. Damrongwiriyanupap, T. Imjai, P. Chaimahawan, P. Sukontasukkul played roles in revising the manuscript. The manuscript has contributions from all authors. All authors discussed the results, reviewed, and approved the final version of the manuscript.

### Acknowledgments

This study was supported by the Thailand Science Research and Innovation Fund and the University of Phayao (Grant No. FF65-RIM079 and FF65-UoE004) and by TRF Senior Research Scholar under Grant RTA 6280012. Furthermore, the authors would also like to thank the anonymous reviewers for their valuable and constructive comments.

### Conflict of Interest

The authors declared no potential conflicts of interest with respect to the research, authorship and publication of this article.

### Funding

Financial support of this work was provided by the Thailand Science Research and Innovation Fund and the University of Phayao (Grant No. FF65-RIM079 and FF65-UoE004) and by TRF Senior Research Scholar under Grant RTA 6280012.

### Data Availability Statements

The datasets generated and/or analyzed during the current study are available from the corresponding author on reasonable request.

### References

- [1] Zhang, J., Makris, N., Seismic response analysis of highway overcrossings including soil-structure interaction, *Earthquake Engineering & Structural Dynamics*, 31(11), 2002, 1967-1991.
- [2] Xie, Y., DesRoches, R., Sensitivity of seismic demands and fragility estimates of a typical California highway bridge to uncertainties in its soil-structure interaction modeling, *Engineering Structures*, 189, 2019, 605-617.
- [3] Katzenbach, R., Leppla, S., Vogler, M., Seip, M., Kurze, S., Soil-structure-interaction of tunnels and superstructures during construction and service time, *Procedia Engineering*, 57, 2013, 35-44.
- [4] Kontogianni, V., Stiros, S.C., Ground loss and static soil-structure interaction during urban tunnel excavation: Evidence from the excavation of the Athens Metro, *Infrastructures*, 5(8), 2020, 64.
- [5] Gharad, A.M., Sonparote, R.S., Influence of soil-structure interaction on the dynamic response of continuous and integral bridge subjected to moving loads, *International Journal of Rail Transportation*, 8(3), 2020, 285-306.
- [6] Östlund, J.L., Andersson, A., Ülker-Kaustell, M., Battini, J.-M., On the influence of shallow soil strata on the dynamic soil-structure interaction of simply supported high-speed railway bridges, *International Journal of Rail Transportation*, 9(5), 2021, 405-423.
- [7] Nguyen, K.T., Reduced-order model for dynamic soil-pipe interaction analysis, Ph.D. Thesis, California institute of technology, Pasadena, California, USA, 2020.
- [8] Jena, S.K., Chakraverty, S., Malikan, M., Sedighi, H.M., Implementation of Hermite-Ritz method and Navier's technique for vibration of functionally graded porous nanobeam embedded in Winkler-Pasternak elastic foundation using bi-Helmholtz nonlocal elasticity, *Journal of Mechanics of Materials and Structures*, 15(3), 2020, 405-434.
- [9] Koochi, A., Goharimanesh, M., Nonlinear oscillations of CNT nano-resonator based on nonlocal elasticity: The energy balance method, *Reports in Mechanical Engineering*, 2(1), 2021, 41-50.
- [10] Abouelregal, A.E., Sedighi, H.M., Faghidian, S.A., Shirazi, A.H., Temperature-dependent physical characteristics of the rotating nonlocal nanobeam subject to a varying heat source and a dynamic load, *Facta Universitatis, Series: Mechanical Engineering*, 19(4), 2021, 633-656.
- [11] Gueguen, P., Bard, P.-Y., Soil-structure and soil-structure-soil interaction: Experimental evidence at the Volvi test site, *Journal of Earthquake Engineering*, 9(5), 2005, 657-693.
- [12] Sapountzakis, E., Kampitsis, A., Inelastic analysis of beams on two-parameter tensionless elastoplastic foundation, *Engineering Structures*, 48, 2013, 389-401.
- [13] Limkatanyu, S., Damrongwiriyanupap, N., Kwon, M., Ponbunyanon, P., Force-based derivation of exact stiffness matrix for beams on Winkler-Pasternak Foundation, *ZAMM Journal of Applied Mathematics and Mechanics: Zeitschrift für Angewandte Mathematik und Mechanik*, 95(2), 2015, 140-155.
- [14] Tabatabaiefar, S.H.R., Fatahi, B., Samali, B., Numerical and experimental investigations on seismic response of building frames under influence of soil-structure interaction, *Advances in Structural Engineering*, 17(1), 2016, 109-130.
- [15] Fathi, A., Sadeghi, A., Azadi, M.R.E., Hoveidae, N., Assessing the soil-structure interaction effects by direct method on the out-of-plane behavior of masonry structures (case study: Arge-Tabriz), *Bulletin of Earthquake Engineering*, 18, 2020, 6429-6443.
- [16] Liu, S., Liu, S., Zhang, W., Lu, Z., Experimental study and numerical simulation on dynamic soil-structure interaction under earthquake excitations, *Soil Dynamics and Earthquake Engineering*, 138, 2020, 106333.
- [17] Yue, F., A refined model for analysis of beams on two-parameter foundations by iterative method, *Mathematical Problems in Engineering*, 2021, 5562212.
- [18] Riaz, M.R., Motoyama, H., Hori, M., Review of soil-structure interaction based on continuum mechanics theory and use of high performance computing, *Geosciences*, 11(2), 2021, 72.
- [19] Schuricht, F., A new mathematical foundation for contact interactions in continuum physics, *Archive for Rational Mechanics and Analysis*, 184, 2007, 495-551.
- [20] Steinmann, P., *Geometrical foundations of continuum mechanics*, Springer, Berlin, Heidelberg, German, 2015.
- [21] Mullapudi, R., Ayoub, A., Nonlinear finite element modeling of beams on two-parameter foundations, *Computers and Geotechnics*, 37(3), 2010, 334-342.
- [22] Limkatanyu, S., Sae-Long, W., Prachasaree, W., Kwon, M., Improved nonlinear displacement-based beam element on a two-parameter foundation, *European Journal of Environmental and Civil Engineering*, 19(6), 2015, 649-671.
- [23] Elishakoff, I., Tonzani, G.M., Zaza, N., Marzani, A., Contrasting three alternative versions of Timoshenko-Ehrenfest theory for beam on Winkler elastic foundation – simply supported beam, *ZAMM Journal of Applied Mathematics and Mechanics: Zeitschrift für Angewandte Mathematik und Mechanik*,



- 98(8), 2018, 1334-1368.
- [24] Tran, Q.A., Villard, P., Dias, D., Discrete and continuum numerical modeling of soil arching between piles, *International Journal of Geomechanics*, 19(2), 2019, 04018195.
- [25] Yavari, A., Sarkani, S., Reddy, J.N., Generalized solutions of beams with jump discontinuities on elastic foundations, *Archive of Applied Mechanics*, 71(9), 2001, 625-639.
- [26] Limkatanyu, S., Kuntiyawichai, K., Spacone, E., Kwon, M., Nonlinear Winkler-based beam element with improved displacement shape functions, *KSCE Journal of Civil Engineering*, 17, 2013, 192-201.
- [27] Papachristou, K.S., Sophianopoulos, D.S., Buckling of beams on elastic foundation considering discontinuous (unbonded) contact, *International Journal of Mechanics and Applications*, 3(1), 2013, 4-12.
- [28] Boudaa, S., Khalfallah, S., Bilotta, E., Static interaction analysis between beam and layered soil using a two-parameter elastic foundation, *International Journal of Advanced Structural Engineering*, 11, 2019, 21-30.
- [29] Sae-Long, W., Limkatanyu, S., Hansapinyo, C., Prachasaree, W., Rungamornrat, J., Kwon, M., Nonlinear flexibility-based beam element on Winkler-Pasternak foundation, *Geomechanics and Engineering*, 24(4), 2021, 371-388.
- [30] Alimoradzadeh, M., Salehi, M., Esfarjani, S.M., Nonlinear dynamic response of an axially functionally graded (AFG) beam resting on nonlinear elastic foundation subjected to moving load, *Nonlinear Engineering*, 8(1), 2019, 250-260.
- [31] Winkler, E., *Die Lehre von der und Festigkeit*, Dominicus, Prague, Czechoslovakia, 1867.
- [32] Filonenko-Borodich, M.M., Some approximate theories of the elastic foundation, *Uchenye Zapiski Moskovskogo Gosudarstvennogo Universiteta Mekhanika*, Moscow, 46, 1940, 3-18.
- [33] Pasternak, P.L., *On a new method of analysis of an elastic foundation by means of two foundation constants*, Gosuderevstvennae Izdatel'sva Literaturi po Stroitel'stvu i Arkhitekture, Moscow, USSR (in Russian), 1954.
- [34] Hetényi, M., *Beams on elastic foundation: Theory with applications in the fields of civil and mechanical engineering*, University of Michigan, USA, 1971.
- [35] Zhaohua, F., Cook, R.D., Beam elements on two-parameter elastic foundations, *Journal of Engineering Mechanics*, 109(6), 1983, 1390-1402.
- [36] Hetényi, M., A general solution for the bending of beams on an elastic foundation of arbitrary continuity, *Journal of Applied Physics*, 21(1), 1950, 55-58.
- [37] Kerr, A.D., A study of a new foundation model, *Acta Mechanica*, 1, 1965, 135-147.
- [38] Limkatanyu, S., Prachasaree, W., Damrongwiriyanupap, N., Kwon, M., Jung, W., Exact stiffness for beams on Kerr-type foundation: The virtual force approach, *Journal of Applied Mathematics*, 2013, 626287.
- [39] Cai, J.B., Chen, W.Q., Ye, G.R., Ding, H.J., On natural frequencies of a transversely isotropic cylindrical panel on a Kerr foundation, *Journal of Sound and Vibration*, 232(5), 2000, 997-1004.
- [40] Avramidis, I.E., Morfidis, K., Bending of beams on three-parameter elastic foundation, *International Journal of Solids and Structures*, 43(2), 2006, 357-375.
- [41] Zhang, L., Wu, G.T., Wu, J., A Kerr-type elastic foundation model for the buckling analysis of a beam bonded on an elastic layer, *ZAMM Journal of Applied Mathematics and Mechanics: Zeitschrift für Angewandte Mathematik und Mechanik*, 99(10), 2019, e201900162.
- [42] Wang, J.-J., Chen, F., Li, D., A simple solution of settlement for low reinforced embankments on Kerr foundation, *Yantu Lixue/Rock and Soil Mechanics*, 40(1), 2019, 250-259.
- [43] Jena, S.K., Chakraverty, S., Malikan, M., Application of shifted Chebyshev polynomial-based Rayleigh-Ritz method and Navier's technique for vibration analysis of a functionally graded porous beam embedded in Kerr foundation, *Engineering with Computers*, 37, 2021, 3569-3589.
- [44] Lynn, A.C., Moehle, J.P., Mahin, S.A., Holmes, W.T., Seismic evaluation of existing reinforced concrete building columns, *Earthquake Spectra*, 12(4), 1996, 715-739.
- [45] Sezen, H., Whittaker, A.S., Elwood, K.J., Mosalam, K.M., Performance of reinforced concrete buildings during the August 17, 1999 Kocaeli, Turkey earthquake, and seismic design and construction practice in Turkey, *Engineering Structures*, 25(1), 2003, 103-114.
- [46] Mergos, P.E., Beyer, K., Modelling shear-flexure interaction in equivalent frame models of slender reinforced concrete walls, *The Structural Design of Tall and Special Buildings*, 23(15), 2014, 1171-1189.
- [47] Feng, N., Fu, C., Seismic behavior of nonductile RC frame slotted with corrugated steel plate shear walls, *Advances in Civil Engineering*, 2021, 6653592.
- [48] Sae-Long, W., Limkatanyu, S., Damrongwiriyanupap, N., Shear-flexure-interaction frame element inclusion of bond-slip effect for seismic analysis of non-ductile RC columns, *Chiang Mai Journal of Science*, 41(1), 2022, 14-26.
- [49] Nouali, A., Matallah, M., A simplified approach to assess the size effect on the shear-flexure interaction in RC elements, *Engineering Structures*, 144, 2017, 151-162.
- [50] Panedpojaman, P., *Design of steel beams and steel beams with openings*, 2<sup>nd</sup> Edition, Songkhla: Faculty of Engineering, Prince of Songkla University (In Thai), 2020.
- [51] Elizalde, H., Cárdenas, D., Delgado-Gutierrez, A., Probst, O., In-plane shear-axial strain coupling formulation for shear-deformable composite thin-walled beams, *Journal of Applied and Computational Mechanics*, 7(2), 2021, 450-469.
- [52] Vecchio, F.J., Collins, M.P., The modified compression field theory for reinforced concrete elements subjected to shear, *ACI Journal*, 83(2), 1986, 219-231.
- [53] Guedes, J., Pinto, A.V., *A numerical model for shear dominated bridge piers*, Proceedings of the Second Italy-Japan Workshop on Seismic Design and Retrofit of Bridges, Rome, Italy, 1997.
- [54] Ceresa, P., Petrini, L., Pinho, R., Flexure-shear fiber beam-column elements for modeling frame structures under seismic loading — state of the art, *Journal of Earthquake Engineering*, 11(sup1), 2007, 46-88.
- [55] Priestley, M.J.N., Seible, F., Calvi, G.M., *Seismic design and retrofit of bridges*, John Wiley & Sons, Inc, 1996.
- [56] Ricles, J.M., Yang, Y.-S., Priestley, M.J.N., Modeling nonductile R/C columns for seismic analysis of bridges, *Journal of Structural Engineering*, 124(4), 1998, 415-425.
- [57] Sezen, H., Moehle, J.P., Shear strength model for lightly reinforced concrete columns, *Journal of Structural Engineering*, 130(11), 2004, 1692-1703.
- [58] Beyer, K., Dazio, A., Priestley, M.J.N., Shear deformations of slender reinforced concrete walls under seismic loading, *ACI Structural Journal*, 108(2), 2011, 167-177.
- [59] Biskinis, D.E., Roupakias, G.K., Fardis, M.N., Degradation of shear strength of reinforced concrete members with inelastic cyclic displacements, *ACI Structural Journal*, 101(6), 2004, 773-783.
- [60] Marini, A., Spacone, E., Analysis of reinforced concrete elements including shear effects, *ACI Structural Journal*, 103(5), 2006, 645-655.
- [61] Martinelli, L., Modeling shear-flexure interaction in reinforced concrete elements subjected to cyclic lateral loading, *ACI Structural Journal*, 105(6), 2008, 675-684.
- [62] Ceresa, P., Petrini, L., Pinho, R., Sousa, R., A fibre flexure-shear model for seismic analysis of RC-framed structures, *Earthquake Engineering & Structural Dynamics*, 38(5), 2009, 565-586.
- [63] Feng, D.-C., Wu, G., Sun, Z.-Y., Xu, J.-G., A flexure-shear Timoshenko fiber beam element based on softened damage-plasticity model, *Engineering Structures*, 140, 2017, 483-497.
- [64] Feng, D.-C., Xu, J., An efficient fiber beam-column element considering flexure-shear interaction and anchorage bond-slip effect for cyclic analysis of RC structures, *Bulletin of Earthquake Engineering*, 16, 2018, 5425-5452.
- [65] Sae-Long, W., Limkatanyu, S., Prachasaree, W., Horpibulsuk, S., Panedpojaman, P., Nonlinear frame element with shear-flexure interaction for seismic analysis of non-ductile reinforced concrete columns, *International Journal of Concrete Structures and Materials*, 13, 2019, 32.
- [66] Sae-Long, W., Limkatanyu, S., Hansapinyo, C., Imjai, T., Kwon, M., Forced-based shear-flexure-interaction frame element for nonlinear analysis of non-ductile reinforced concrete columns, *Journal of Applied and Computational Mechanics*, 6, 2020, 1151-1167.
- [67] Mergos, P.E., Kappos, A.J., A distributed shear and flexural flexibility model with shear-flexure interaction for R/C members subjected to seismic loading, *Earthquake Engineering & Structural Dynamics*, 37(12), 2008, 1349-1370.
- [68] Mergos, P.E., Kappos, A.J., A gradual spread inelasticity model for R/C beam-columns, accounting for flexure, shear and anchorage slip, *Engineering Structures*, 44, 2012, 94-106.
- [69] Sae-Long, W., Limkatanyu, S., Panedpojaman, P., Prachasaree, W., Damrongwiriyanupap, N., Kwon, M., Hansapinyo, C., Nonlinear Winkler-based frame element with inclusion of shear-flexure interaction effect for analysis of non-ductile RC members on foundation, *Journal of Applied and Computational Mechanics*, 7(1), 2021, 148-164.



- [70] Carrera, E., Giunta, G., Petrolo, M., *Beam structures: Classical and advanced theories*, John Wiley & Sons, Ltd., 2011.
- [71] Taylor, R.L., *FEAP: A finite element analysis program*, User manual: version 7.3, Department of Civil and Environmental Engineering, University of California, Berkeley, USA, 2000.
- [72] Kent, D.C., Park, R., Flexural members with confined concrete, *Journal of the Structural Division*, 97(7), 1971, 1964-1990.
- [73] Menegotto, M., Pinto, P.E., Method of analysis for cyclically loaded reinforced concrete plane frames including changes in geometry and nonelastic behavior of elements under combined normal force and bending, *Proceeding of IABSE Symposium on Resistance and Ultimate Deformability of Structures Acted on by Well-Defined Repeated Loads*, Lisbon, 1973, 15-22.
- [74] Spacone, E., Limkatanyu, S., Responses of reinforced concrete members including bond-slip effects, *ACI Structural Journal*, 97(6), 2000, 831-839.
- [75] Rakowski, J., The interpretation of the shear locking in beam elements, *Computers & Structures*, 37(5), 1990, 769-776.
- [76] Beirao da Veiga, L., Lovadina, C., Reali, A., Avoiding shear locking for the Timoshenko beam problem via isogeometric collocation methods, *Computer Methods in Applied Mechanics and Engineering*, 241-244, 2012, 38-51.
- [77] Lee, S.J., Park, K., Static analysis of Timoshenko beams using isogeometric approach, *Architectural Research*, 16(2), 2014, 57-65.
- [78] Baier-Saip, J.A., Baier, P.A., de Faria, A.R., Oliveira, J.C., Baier, H., Shear locking in one-dimensional finite element methods, *European Journal of Mechanics / A Solids*, 79, 2020, 103871.
- [79] Priestley, M.J.N., Seible, F., Verma, R., Xiao, Y., Seismic shear strength of reinforced concrete columns, *Structural Systems Research Project Report No. SSRP 93/06*, University of California, San Diego, USA, 1993.
- [80] Park, R., Paulay, T., *Reinforced concrete structures*, John Wiley & Sons, New York, USA, 1975.
- [81] Sezen, H., *Seismic behavior and modeling of reinforced concrete building columns*, Ph.D. Thesis, Department of Civil and Environmental Engineering, University of California, Berkeley, USA, 2002.
- [82] Lynn, A.C., *Seismic evaluation of existing reinforced concrete building columns*, Ph.D. Thesis, Department of Civil and Environmental Engineering, University of California, Berkeley, USA, 2001.
- [83] Antonio, L.M., Pavanello, R., de Almeida Barros, P.L., Marine pipeline-seabed interaction modeling based on Kerr-type foundation, *Applied Ocean Research*, 80, 2018, 228-239.
- [84] Shiri, H., Response of steel catenary risers on hysteretic non-linear seabed, *Applied Ocean Research*, 44, 2014, 20-28.
- [85] Alemdar, B.N., Güllkan, P., Beams on generalized foundations: supplementary element matrices, *Engineering Structures*, 19(11), 1997, 910-920.
- [86] Morfidis, K., Exact matrices for beams on three-parameter elastic foundation, *Computers & Structures*, 85(15-16), 2007, 1243-1256.

## ORCID iD

Suchart Limkatanyu  <https://orcid.org/0000-0002-4343-7654>  
 Worathep Sae-Long  <https://orcid.org/0000-0001-8149-4409>  
 Nattapong Damrongwiriyanupap  <https://orcid.org/0000-0001-7280-5957>  
 Thanongsak Imjai  <https://orcid.org/0000-0002-3220-7669>  
 Preeda Chaimahawan  <https://orcid.org/0000-0002-3515-0506>  
 Piti Sukontasukkul  <https://orcid.org/0000-0002-9580-7063>



© 2022 Shahid Chamran University of Ahvaz, Ahvaz, Iran. This article is an open access article distributed under the terms and conditions of the Creative Commons Attribution-NonCommercial 4.0 International (CC BY-NC 4.0 license) (<http://creativecommons.org/licenses/by-nc/4.0/>).

**How to cite this article:** Limkatanyu S., Sae-Long W., Damrongwiriyanupap N., Imjai T., Chaimahawan P., Sukontasukkul P. Shear-flexure Interaction Frame Model on Kerr-type Foundation for Analysis of Non-ductile RC Members on Foundation, *J. Appl. Comput. Mech.*, 8(3), 2022, 1076-1090. <https://doi.org/10.22055/jacm.2022.39597.3440>

**Publisher's Note** Shahid Chamran University of Ahvaz remains neutral with regard to jurisdictional claims in published maps and institutional affiliations.

